New Numerical Methods to Evaluate Homogeneous Solutions of the Teukolsky Equation. II

—— *Solutions of the Continued Fraction Equation* ——

Ryuichi FUJITA and Hideyuki TAGOSHI

Department of Earth and Space Science, Graduate School of Science,
Osaka University, Toyonaka 560-0043, Japan

We investigate the solution of the continued fraction equation by which we determine "the renormalized angular momentum parameter", ν, in the formalism developed by Leaver and Mano, Suzuki and Takasugi. In this formalism, we describe the homogeneous solutions of the radial Teukolsky equation, which is the basic equation of the black hole perturbation formalism. We find that, contrary to the assumption made in previous works, the solution, ν, becomes complex valued as ω (the angular frequency) becomes large for each l and m (the degree and order of the spin-weighted spheroidal harmonics). We compare the power radiated by gravitational waves from a particle in a circular orbit in the equatorial plane around a Kerr black hole in two ways, one using the Mano-Suzuki-Takasugi formalism with complex ν and the other using a direct numerical integration method. We find that the two methods produce consistent results. These facts prove the validity of using complex solutions to determine the homogeneous solutions of the Teukolsky equation.

§1. Introduction

Inspirals of stellar-mass compact objects into a supermassive black hole at galactic nuclei are expected to be one of the most important sources of gravitational waves for space-based detectors, such as the Laser Interferometer Space Antenna (LISA).[1],[2] Through the observation of gravitational waves from such systems, we may be able to obtain information regarding the central black hole's spacetime geometry encoded in multipole moments. We may also obtain astrophysical information, such as the mass distribution of compact objects in galactic nuclei. Theoretical waveforms of gravitational waves from such systems are required in order to extract such information through data analysis.

To predict the waveforms of extreme mass ratio inspirals, we adopt the black hole perturbation approach. In this approach, a compact star is treated as a point particle, and the mass of the compact star, μ, is assumed to be very small compared to the mass of the black hole, M, i.e. $\mu/M \ll 1$. In this context, the Teukolsky equation[3] describes the evolution of a perturbation of the Kerr black hole spacetime. The standard approach to solve the Teukolsky equation is based on the Green function method. The Green function is constructed from two kinds of homogeneous solutions. The solution of the Teukolsky equation is obtained by the integration of the Green function multiplied by the source term.

In a previous paper[4] (paper I), we discussed a numerical method to evaluate the homogeneous solutions using a formalism developed by Mano et al.[5] (MST). In this

formalism, homogeneous solutions are expressed in series of hypergeometric functions around the horizon and in series of Coulomb wave functions around infinity. This formalism is an extension of the formalism of Leaver,[6] in which only the series of Coulomb wave functions are given. One of the most important problems in the application of the Leaver and the MST formalisms to numerical computation is to determine the so-called "renormalized angular momentum", ν, by solving an equation of the form $g(\nu) = 0$, where $g(\nu)$ is expressed in terms of continued fractions. We found that, for each s, ℓ, m and q (where s is the spin index of the Teukolsky equation, ℓ and m are the indices of the spin weighted spheroidal harmonics, and q is the Kerr parameter divided by the mass of the black hole, $q = a/M$), there is a maximum value of ω for which we can obtain ν, if we assume that the ν is real.

In this paper, we investigate in more detail the properties of the solution of the continued fraction equation $g(\nu) = 0$, defined in the Leaver and the MST formalisms. We search for ν in the complex region if we cannot find ν in the real region. We find that the solution is actually complex valued when no real solutions are found. Further, we find that the real part of the complex solutions, when they exist, always take integer or half-integer values. We confirm that these complex solutions of the continued fraction equation can be used to determine the homogeneous solutions of the Teukolsky equation. We compare the power radiated by gravitational waves from a particle in a circular orbit in the equatorial plane around a Kerr black hole computed by the MST formalism with complex ν and by a direct numerical integration method. We find that the two methods give consistent results. These facts show the validity of using the complex solutions to determine the homogeneous solutions of the Teukolsky equation. By using complex ν, we can evaluate gravitational waves even in the case that $M\omega$ becomes large. This range of $M\omega$ is important for the LISA data analysis which deals with the case that a particle moves in the strong gravitational field or more generic orbits.

This paper is organized as follows. In §2, we briefly review the MST formalism and introduce the continued fraction equation, $g(\nu) = 0$. In §3, we discuss the properties of the solutions of the continued fraction equation. In §4, we compare the power radiated by gravitational waves from a particle around a Kerr black hole computed by the MST formalism and by a direct numerical integration method. Section 5 is devoted to a summary and discussion. Throughout this paper, we use units in which $G = c = 1$.

§2. Analytic solutions of the homogeneous Teukolsky equation, and the continued fraction equation

In this paper, we consider only the case $\omega \geq 0$. Solutions in the case $\omega < 0$ can be obtained from those in the case $\omega > 0$ by the symmetry of the Teukolsky equation.

The homogeneous Teukolsky equation is given by

$$\Delta^2 \frac{d}{dr} \left(\frac{1}{\Delta} \frac{dR_{\ell m \omega}}{dr} \right) - V(r) R_{\ell m \omega} = 0, \tag{2.1}$$

where the potential term $V(r)$ is given by

$$V(r) = -\frac{K^2 + 4i(r-M)K}{\Delta} + 8i\omega r + \lambda. \tag{2.2}$$

Here $\Delta = r^2 - 2Mr + a^2 = (r - r_+)(r - r_-)$, with $r_\pm = M \pm \sqrt{M^2 - a^2}$ and $K = (r^2 + a^2)\omega - ma$, and λ is the eigenvalue of the angular Teukolsky equation.

We consider the incoming solution of the homogeneous Teukolsky equation defined by the asymptotic behavior

$$R_{lm\omega}^{\text{in}} \to \begin{cases} B_{lm\omega}^{\text{trans}} \Delta^2 e^{-ikr*} & \text{for } r \to r_+, \\ r^3 B_{lm\omega}^{\text{ref}} e^{i\omega r*} + r^{-1} B_{lm\omega}^{\text{inc}} e^{-i\omega r*} & \text{for } r \to +\infty, \end{cases} \tag{2.3}$$

where $k = \omega - ma/2Mr_+$ and r^* is the tortoise coordinate defined by

$$r^* = r + \frac{2Mr_+}{r_+ - r_-} \ln \frac{r - r_+}{2M} - \frac{2Mr_-}{r_+ - r_-} \ln \frac{r - r_-}{2M}. \tag{2.4}$$

Here $r_\pm = M \pm \sqrt{M^2 - a^2}$.

In the MST method, the homogeneous solutions of the Teukolsky equation are expressed in terms of two kinds of series of special functions.[5),7)] One consists of series of hypergeometric functions, and the other consists of series of Coulomb wave functions. The former is convergent at the horizon, while the latter at infinity.

For the homogeneous solution, $R_{lm\omega}^{\text{in}}$, we define p_{in} by

$$R^{\text{in}} = e^{i\epsilon\kappa x}(-x)^{-s-i(\epsilon+\tau)/2}(1-x)^{i(\epsilon-\tau)/2}p_{\text{in}}(x). \tag{2.5}$$

The function p_{in} is expressed in the form of a series of hypergeometric functions as

$$p_{\text{in}}(x) = \sum_{n=-\infty}^{\infty} a_n F(n + \nu + 1 - i\tau, -n - \nu - i\tau; 1 - s - i\epsilon - i\tau; x), \tag{2.6}$$

where $x = \omega(r_+ - r)/\epsilon\kappa$, $\epsilon = 2M\omega$, $\kappa = \sqrt{1 - q^2}$, $q = a/M$ and $\tau = (\epsilon - mq)/\kappa$, and $F(\alpha, \beta; \gamma; x)$ is the hypergeometric function.

Next, we present a solution in the form of a series of Coulomb wave functions. Let us denote a homogeneous solution by R_C. We define the function $f_\nu(z)$ through the relation

$$R_C = z^{-1-s}\left(1 - \frac{\epsilon\kappa}{z}\right)^{-s-i(\epsilon+\tau)/2} f_\nu(z). \tag{2.7}$$

We express the function $f_\nu(z)$ in the form of a series of Coulomb wave functions as

$$f_\nu(z) = \sum_{n=-\infty}^{\infty} (-i)^n \frac{(\nu + 1 + s - i\epsilon)_n}{(\nu + 1 - s + i\epsilon)_n} a_n F_{n+\nu}(-is - \epsilon, z), \tag{2.8}$$

where $z = \omega(r - r_-)$ and $(a)_n = \Gamma(a + n)/\Gamma(a)$, and $F_N(\eta, z)$ is a Coulomb wave function defined by

$$F_N(\eta, z) = e^{-iz}2^N z^{N+1} \frac{\Gamma(N + 1 - i\eta)}{\Gamma(2N + 2)} \Phi(N + 1 - i\eta, 2N + 2; 2iz). \tag{2.9}$$

Here $\Phi(\alpha, \beta; z)$ is the confluent hypergeometric function, which is regular at $z = 0$ (see §13 of Ref. 8)). The function R_{C} is related to R^{in} by

$$R^{\mathrm{in}} = K_\nu R_{\mathrm{C}}^\nu + K_{-\nu-1} R_{\mathrm{C}}^{-\nu-1}, \tag{2·10}$$

where K_ν is given by Eq. (2·20) of paper I.

The expansion coefficients of the series of hypergeometric functions and the series of Coulomb wave functions, $\{a_n\}$, satisfy the same three-term recurrence relation, given by

$$\alpha_n^\nu a_{n+1} + \beta_n^\nu a_n + \gamma_n^\nu a_{n-1} = 0, \tag{2·11}$$

where

$$\begin{aligned}
\alpha_n^\nu &= i\epsilon\kappa(n + \nu)(2n + 2\nu - 1)(n + \nu + 1 + s + i\epsilon) \\
&\quad \times (n + \nu + 1 + s - i\epsilon)(n + \nu + 1 + i\tau),
\end{aligned} \tag{2·12}$$

$$\begin{aligned}
\beta_n^\nu &= \bigl(-\lambda - s(s + 1) + (n + \nu)(n + \nu + 1) + \epsilon^2 + \epsilon(\epsilon - mq)\bigr) \\
&\quad \times (n + \nu)(n + \nu + 1)(2n + 2\nu + 3)(2n + 2\nu - 1) \\
&\quad + \epsilon(\epsilon - mq)(s^2 + \epsilon^2)(2n + 2\nu + 3)(2n + 2\nu - 1),
\end{aligned} \tag{2·13}$$

$$\begin{aligned}
\gamma_n^\nu &= -i\epsilon\kappa(n + \nu + 1)(2n + 2\nu + 3)(n + \nu - s + i\epsilon) \\
&\quad \times (n + \nu - s - i\epsilon)(n + \nu - i\tau).
\end{aligned} \tag{2·14}$$

The definitions of $\alpha_n^\nu, \beta_n^\nu$ and γ_n^ν are different from those given in paper I by the factor $(n + \nu)(n + \nu + 1)(2n + 2\nu + 3)(2n + 2\nu - 1)$. The series of Coulomb wave functions and the three term recurrence relation Eq. (2·11) are equivalent to those obtained by Leaver.[6]

We note that the parameter ν introduced in the above formulas does not exist in the Teukolsky equation. This parameter is introduced so that both series converge and actually represent a solution of the Teukolsky equation. Here, we review the method to determine ν and obtain the convergence of both series expansions, based on Ref. 9).

There are two independent solutions of Eq. (2·11) whose asymptotic behavior for $n \to \infty$ is given by

$$\lim_{n \to \infty} n \frac{a_n^{(1)}}{a_{n-1}^{(2)}} = \frac{i\epsilon\kappa}{2}, \quad \lim_{n \to \infty} \frac{a_n^{(2)}}{n a_{n-1}^{(2)}} = \frac{2i}{\epsilon\kappa}. \tag{2·15}$$

There are also two independent solutions whose asymptotic behavior for $n \to -\infty$ is given by

$$\lim_{n \to -\infty} n \frac{a_n^{(3)}}{a_{n-1}^{(3)}} = -\frac{i\epsilon\kappa}{2}, \quad \lim_{n \to -\infty} \frac{a_n^{(4)}}{n a_{n-1}^{(4)}} = -\frac{2i}{\epsilon\kappa}. \tag{2·16}$$

It is shown that in order to have convergence of Eqs. (2·6) and (2·8), the coefficients, $a_n^{(1)}$, must be used for $n \to \infty$, and the coefficients $a_n^{(3)}$ must be used for $n \to -\infty$. These two solutions are called the "minimal solution" as $n \to \pm\infty$, respectively.

In fact, it can be proved that if we use these solutions as the expansion coefficients $\{a_n\}$, the series of hypergeometric functions Eq. (2·6) converges for x in the range $-\infty < x \le 0$, and the series Eq. (2·8) converges for $z > \epsilon\kappa$, or equivalently, $r > r_+$. However, these two solutions do not coincide in general. In order to obtain a consistent solution, the parameter ν is used.

We next introduce the following quantities:

$$R_n \equiv \frac{a_n^{(1)}}{a_{n-1}^{(1)}}, \quad L_n \equiv \frac{a_n^{(3)}}{a_{n+1}^{(3)}}. \tag{2·17}$$

We can express R_n and L_n in terms of continued fractions as

$$
\begin{aligned}
R_n &= -\frac{\gamma_n^\nu}{\beta_n^\nu + \alpha_n^\nu R_{n+1}} \\
&= -\frac{\gamma_n^\nu}{\beta_n^\nu -} \frac{\alpha_n^\nu \gamma_{n+1}^\nu}{\beta_{n+1}^\nu -} \frac{\alpha_{n+1}^\nu \gamma_{n+2}^\nu}{\beta_{n+2}^\nu -} \cdots,
\end{aligned} \tag{2·18}
$$

$$
\begin{aligned}
L_n &= -\frac{\alpha_n^\nu}{\beta_n^\nu + \gamma_n^\nu L_{n-1}} \\
&= -\frac{\alpha_n^\nu}{\beta_n^\nu -} \frac{\alpha_{n-1}^\nu \gamma_n^\nu}{\beta_{n-1}^\nu -} \frac{\alpha_{n-2}^\nu \gamma_{n-1}^\nu}{\beta_{n-2}^\nu -} \cdots.
\end{aligned} \tag{2·19}
$$

The convergence of the above continued fractions is guaranteed, because $\{a_n^{(1)}\}$ and $\{a_n^{(3)}\}$ constitute minimal solutions.[10]

In order to have the coincidence of the two solutions $\{a_n^{(1)}\}$ and $\{a_n^{(3)}\}$, we impose the relation

$$R_n L_{n-1} = 1. \tag{2·20}$$

If we choose ν such that this implicit equation is satisfied for a certain n, we can obtain a minimal solution $\{a_n\}$ that is valid over the entire range $-\infty < n < \infty$.

In place of Eq. (2·20), we define an equivalent equation. First we divide Eq. (2·11) by a_n and replace a_n/a_{n-1} by R_n and a_n/a_{n+1} by L_n. We then find

$$g_n(\nu) \equiv \beta_n^\nu + \alpha_n^\nu R_{n+1} + \gamma_n^\nu L_{n-1} = 0, \tag{2·21}$$

where R_{n+1} and L_{n-1} are given by the continued fractions Eqs. (2·18) and (2·19), respectively. Equation (2·21) is a transcendental equation expressed in terms of continued fractions. We call Eq. (2·21) the "continued fraction equation" in this paper.

§3. Properties of the solutions of the continued fraction equation

We first note that $g_n(\nu)$ in Eq. (2·21) is invariant under the simultaneous transformation $\nu \leftrightarrow -\nu - 1$ and $n \leftrightarrow -n$. Thus, $g_0(\nu)$ is symmetric under $\nu \leftrightarrow -\nu - 1$. In particular, if we plot $g_0(\nu)$ as a function of ν, $g_0(\nu)$ is symmetric about the line $\nu = -1/2$ in the complex plane.

Next, we note that the coefficients α_n^ν, β_n^ν and γ_n^ν in Eqs. (2·12) – (2·14) contain ν only in the form $n + \nu$. This implies that $g_n(\nu+1) = g_{n+1}(\nu)$. When ν is a solution of Eq. (2·21), we have $g_n(\nu) = 0$. This can be rewritten as

$$g_{n+1}(\nu) = \beta_{n+1} + \alpha_{n+1} R_{n+2} + \gamma_{n+1} L_n = 0.$$

We then have $0 = g_{n+1}(\nu) = g_n(\nu + 1)$. Thus, $\nu + 1$ is also a solution. Namely, if $g_n(\nu) = 0$, $g_n(\nu + k) = 0$ for an arbitrary integer k. These considerations show that it is sufficient to investigate $g_0(\nu) = 0$ to find the solution ν.

When $\epsilon = 2M\omega$ is small, there is an analytic expression of a solution ν in the form of a series in ϵ, given by

$$\nu = l + \frac{1}{2l+1}\left[-2 - \frac{s^2}{l(l+1)} + \frac{[(l+1)^2 - s^2]^2}{(2l+1)(2l+2)(2l+3)}\right.$$
$$\left. - \frac{(l^2 - s^2)^2}{(2l-1)2l(2l+1)}\right]\epsilon^2 + O(\epsilon^3). \tag{3·1}$$

Thus, when $\epsilon \to 0$, ν takes an integer value $\nu = l + k$ (where k is an arbitrary integer). As an example, we consider the case $l = m = 2$, $q = 0$ and $k = 0$. Then, as ω increases from 0, the solution ν decreases from l and approaches $l - 1/2$ near $M\omega = 0.36$. If $M\omega$ is larger than 0.36, the real solution ν disappears. The plot of $g_0(x)/l^5$ is shown in Fig. 1 in the case $M\omega \leq 0.36$ and in Fig. 2 in the case $M\omega > 0.36$. The factor l^{-5} is introduced so that the function $g_0(x)/l^5$ remains order unity. At first glance, in Fig. 2, there seems to be a solution at $x = l - 1/2 = 3/2$, $x = 1$ or $x = 2$. However, at these points, $g_0(x)$ always becomes 0, irrespective of ω. These are solutions of $g_0(x) = 0$ mathematically, but they are not solutions that can be used to connect two minimal solutions in the limits $n = \pm\infty$, discussed in the previous section. In Table I of paper I, we listed the maximum values of $M\omega$ for which real ν is found. We also list them in Table I for convenience. We express the maximum value of $M\omega$ as $(M\omega)_{\max}$.

Next we consider the solution of $g_0(z) = 0$ in the complex z plane in the case that $M\omega$ is larger than $(M\omega)_{\max}$ and we cannot find a real solution. In Fig. 3, we plot a contour of $|g_0(z)|$ in the case $M\omega = 0.5$. We find that there is a minimum near $\mathrm{Re}(z) = 3/2$, $\mathrm{Im}(z) = 0.36$. In Fig. 4, we plot $\mathrm{Re}(g_0(z))$ and $\mathrm{Im}(g_0(z))$ as functions of $\mathrm{Im}(z)$ at $\mathrm{Re}(z) = 3/2$. It is evident that there is a solution near $z = 3/2 + 0.36i$. The precise value of the solution is $z = 3/2 + 0.36188061539416i$. It is also suggested by Fig. 3 that there are no solutions other than this value. We find that when there are no real solutions, a complex solution always exists. Further, the real part of the complex solution is always a half-integer or integer. These properties are the same when the parameters, s, l, m and q have different values.

We consider the case in which $M\omega$ is much larger than $(M\omega)_{\max}$. In Table II, we list numerical values of the solution ν in the case $s = -2$, $l = m = 2$ and $q = 0$. We find that $\mathrm{Im}(\nu)$ increases as $M\omega$ increases, and it reaches a maximum value near $M\omega = 0.53$. Then, $\mathrm{Im}(\nu)$ begins to decrease and approaches 0, and the real solution appears again at $M\omega = 0.594$. This new real solution starts at the half integer value $\nu = 3/2$, and it approaches the integer value $\nu = 2$. At $M\omega = 0.604$, where the
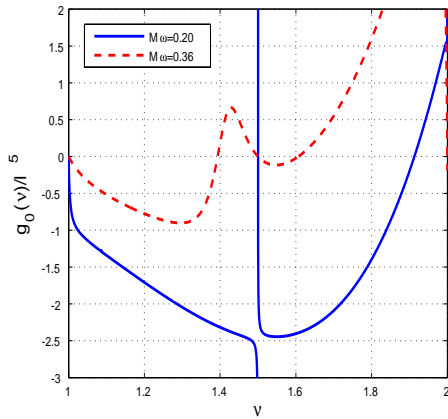
Fig. 1. The plot of $g_0(x)/l^5$ for $M\omega = 0.20$ and 0.36. Here $s = -2$, $l = m = 2$ and $q = 0$. There exist real solutions in these cases.
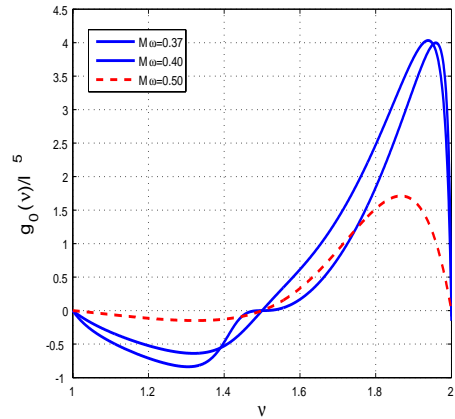

Fig. 2. The plot of $g_0(x)/l^5$ for $M\omega = 0.37$, 0.40 and 0.50. Here $s = -2$, $l = m = 2$ and $q = 0$. No real solutions are found in these cases.
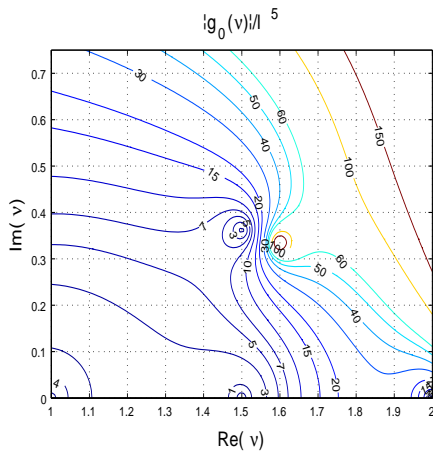

Fig. 3. The contour plot of $|g_0(z)|/l^5$ in the case $M\omega = 0.50$, $s = -2$, $l = m = 2$ and $q = 0$. There is a complex solution at $\nu = 1.5 + 0.36188061539416i$.
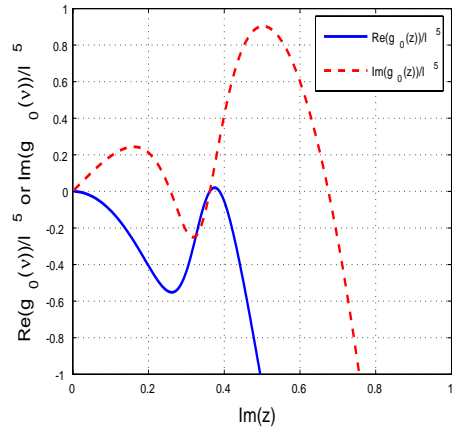

Fig. 4. The real and imaginary parts of the function $g_0(z)/l^5$ at $\mathrm{Re}(z) = 1.5$ in the case $M\omega = 0.50$, $s = -2$, $l = m = 2$ and $q = 0$. The real and imaginary parts become 0 simultaneously at $\mathrm{Im}(z) = 0.36188061539416$. Thus, this function satisfies $g_0(z) = 0$.

real solution reaches $\nu = 2$, the real solution disappears, and the imaginary part appears again. In Table III, we list numerical values of the solution ν in the case $s = -2$, $l = m = 2$ and $q = \pm0.99$. When $q = 0.99$, the real solution disappears at $M\omega = 0.39$, and a complex solution with $\mathrm{Re}(\nu) = 3/2$ appears. Then $\mathrm{Im}(\nu)$ continues to increase until $M\omega = 3.0$. When $q = -0.99$, the real solution disappears at $M\omega = 0.33$, and a complex solution with $\mathrm{Re}(\nu) = 3/2$ appears. Then $\mathrm{Im}(\nu)$

Table I. Maximum values of $M\omega$ for which real solutions ν are found.

ℓ	m	$q = 0.9$	$q = 0$	$q = -0.9$	ℓ	m	$q = 0.9$	$q = 0$	$q = -0.9$
2	2	0.39	0.36	0.32	8	8	1.08	1.00	0.92
2	1	0.44	0.36	0.34	8	7	1.07	1.00	0.93
2	0	0.38	0.36	0.38	8	6	1.06	1.00	0.94
3	3	0.58	0.53	0.45	8	5	1.05	1.00	0.95
3	2	0.61	0.53	0.48	8	4	1.04	1.00	0.96
3	1	0.59	0.53	0.51	8	3	1.03	1.00	0.97
3	0	0.55	0.53	0.55	8	2	1.02	1.00	0.98
4	4	0.73	0.66	0.57	8	1	1.01	1.00	0.99
4	3	0.73	0.66	0.60	8	0	1.00	1.00	1.00
4	2	0.72	0.66	0.63	9	9	1.14	1.06	0.99
4	1	0.70	0.66	0.65	9	8	1.13	1.06	1.00
4	0	0.68	0.66	0.68	9	7	1.12	1.06	1.00
5	5	0.84	0.77	0.68	9	6	1.12	1.06	1.01
5	4	0.83	0.77	0.70	9	5	1.11	1.06	1.02
5	3	0.82	0.77	0.72	9	4	1.10	1.06	1.03
5	2	0.80	0.77	0.74	9	3	1.09	1.06	1.04
5	1	0.79	0.77	0.76	9	2	1.08	1.06	1.05
5	0	0.77	0.77	0.77	9	1	1.07	1.06	1.06
6	6	0.93	0.85	0.77	9	0	1.06	1.06	1.06
6	5	0.92	0.85	0.79	10	10	1.20	1.12	1.05
6	4	0.91	0.85	0.80	10	9	1.19	1.12	1.05
6	3	0.89	0.85	0.82	10	8	1.19	1.12	1.06
6	2	0.88	0.85	0.83	10	7	1.18	1.12	1.07
6	1	0.87	0.85	0.84	10	6	1.17	1.12	1.08
6	0	0.86	0.85	0.86	10	5	1.16	1.12	1.09
7	7	1.01	0.93	0.85	10	4	1.16	1.12	1.09
7	6	1.00	0.93	0.86	10	3	1.15	1.12	1.10
7	5	0.99	0.93	0.88	10	2	1.14	1.12	1.11
7	4	0.98	0.93	0.89	10	1	1.13	1.12	1.12
7	3	0.96	0.93	0.90	10	0	1.12	1.12	1.12
7	2	0.95	0.93	0.91					
7	1	0.94	0.93	0.92					
7	0	0.93	0.93	0.93					

continues to increase until $M\omega = 3.0$. In Tables II and III, we list values for the case $M\omega \leq 3.0$. Above this value, it becomes difficult to evaluate the continued fraction equation numerically, because of the loss of precision. This happens because as $M\omega$ becomes large, β_n approaches $-(\alpha_n^\nu R_{n+1} + \gamma_n^\nu L_{n-1})$ irrespective of ν.

In Figs. 5–13, we plot the real and imaginary parts of ν for $l = m = 2, 3, 4$ and $q = 0, \pm 0.99$. In Figs. 14 and 15, we plot the real and imaginary parts of ν for $l = 2, \cdots, 9$ in the case $q = 0$. We find that the properties of ν are very similar to those in the case $l = 2$, although there are several quantitative differences. For example, in the case $l = 5$, in Figs. 14 and 15, Re(ν) reaches 4.5 at $M\omega = 0.776$, and a complex solution appears. However, this complex solution exists only in a very small interval of $M\omega$, $0.776 \leq M\omega \leq 0.778$, and a real solution appears again for $M\omega > 0.778$.

In Tables IV–VI, we list the values of ν for various $M\omega$ in the cases $s = 0$, $l = m = 2$ and $q = 0, \pm 0.99$. We find behavior of ν very similar to that in the case $s = -2$.

Here, we briefly explain our numerical method of searching for a solution of $g_0(z) = 0$. When we search for a real solution, it should be sufficient, in principle, to search the region $l - 1/2 < x < l$, because of the symmetry property of the solution mentioned above. However, in some cases, the function $g_0(x)$ becomes very steep around the solution in that region. In such cases, it is often easier to search for the solution in the region $l - 1 < x < l - 1/2$. We thus search the region $l - 1 < x < l$. We discard solutions at integer and half-integer values, $x = l - 1, l - 1/2, l$.

When we do not find any solutions on the real z axis, we search for a solution in the imaginary direction. We consider only half-integer and integer values of $\mathrm{Re}(z)$, and search in the imaginary direction of the z-plane. Thus, the problem becomes a simple one-dimensional search for a root of the complex equation $g_0(z) = 0$. Further, we utilize a very useful property of $g_0(z)$: The function $g_0(z)$ (with complex z) is real when $z = -1/2 + iy$ (with real variable y). This is derived using the fact that $\beta_k = \beta_{-k}^*$ and $\alpha_k \gamma_{k+1} = (\alpha_{-k-1}\gamma_{-k})^*$ (where $*$ denotes complex conjugation, and k is an arbitrary integer). Thus, when we search for a solution with half-integer real part, it is convenient to search at $\mathrm{Re}(z) = -1/2$, since when ν is a solution, $\nu + k$ (with k an arbitrary integer) is also a solution. For a solution with integer real part, we search for a solution which simultaneously satisfies $\mathrm{Re}(g_0(z)) = 0$ and $\mathrm{Im}(g_0(z)) = 0$. In particular, we search for the real part

Table II. Table of ν for various values of $M\omega$ in the case $s = -2$, $l = m = 2$ and $q = 0$.

| $M\omega$	$\mathrm{Re}(\nu)$	$\mathrm{Im}(\nu)$
0.1000	1.9793154547208	0.0000000000000
0.2000	1.9129832302687	0.0000000000000
0.3000	1.7792805424199	0.0000000000000
0.3100	1.7594378913945	0.0000000000000
0.3200	1.7375329132632	0.0000000000000
0.3300	1.7129796083608	0.0000000000000
0.3400	1.6847877144372	0.0000000000000
0.3500	1.6510165965479	0.0000000000000
0.3600	1.6066167352463	0.0000000000000
0.3700	1.5000000000000	0.0117805002266
0.3800	1.5000000000000	0.1080591170505
0.4000	1.5000000000000	0.1862468531447
0.4200	1.5000000000000	0.2393542510924
0.4400	1.5000000000000	0.2810676246093
0.4600	1.5000000000000	0.3149109523037
0.4800	1.5000000000000	0.3419264795996
0.5000	1.5000000000000	0.3618806153941
0.5200	1.5000000000000	0.3732918843902
0.5300	1.5000000000000	0.3748108599871
0.5400	1.5000000000000	0.3725753632958
0.5600	1.5000000000000	0.3508153681782
0.5800	1.5000000000000	0.2767032401575
0.5920	1.5000000000000	0.1112238120363
0.5930	1.5000000000000	0.0654237590662
0.5940	1.5671748369160	0.0000000000000
0.5960	1.6572267840117	0.0000000000000
0.5980	1.7231093132436	0.0000000000000
0.6000	1.7878302655744	0.0000000000000
0.6020	1.8649828581648	0.0000000000000
0.6030	1.9221344236998	0.0000000000000
0.6040	2.0000000000000	0.0739848339575
0.6060	2.0000000000000	0.1644030708573
0.6080	2.0000000000000	0.2167770350574
0.7000	2.0000000000000	0.8003377636925
0.8000	2.0000000000000	1.1099466644118
0.9000	2.0000000000000	1.3699138540831
1.0000	2.0000000000000	1.6085538776570
1.2000	2.0000000000000	2.0541150948294
1.4000	2.0000000000000	2.4772658891494
1.6000	2.0000000000000	2.8879097347262
1.8000	2.0000000000000	3.2903727081665
2.0000	2.0000000000000	3.6867890278893
2.2000	2.0000000000000	4.0782125805902
2.4000	2.0000000000000	4.4650426712959
2.6000	2.0000000000000	4.8471678988185
2.8000	2.0000000000000	5.2239336390821
3.0000	2.0000000000000	5.5939000509184
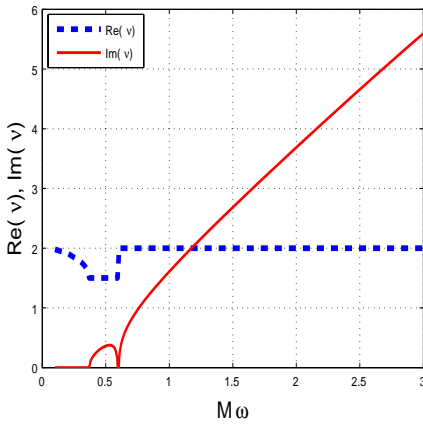
Fig. 5. The values of the real and imaginary parts of ν as functions of $M\omega$ in the case $s = -2$, $l = m = 2$ and $q = 0$.
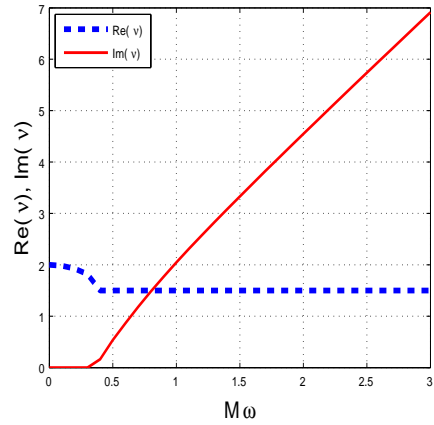

Fig. 6. The values of the real and imaginary parts of ν as functions of $M\omega$ in the case $s = -2$, $l = m = 2$ and $q = 0.99$.
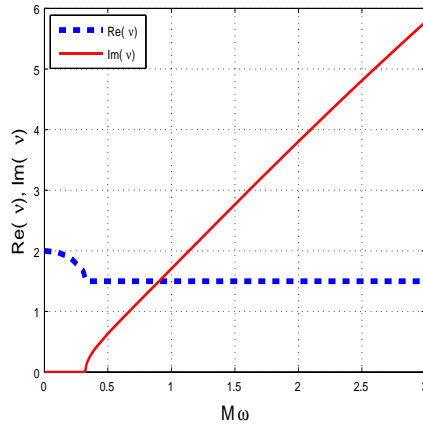

Fig. 7. The values of the real and imaginary parts of ν as functions of $M\omega$ in the case $s = -2$, $l = m = 2$ and $q = -0.99$.

$\mathrm{Re}(z) = 1$ irrespective of l, because the function $g_0(z)$ becomes steeper around the solution as $\mathrm{Re}(z)$ becomes larger, and it becomes more difficult to find the solution in such cases.

§4. Gravitational wave luminosity

Since the role of ν is to match two minimal solutions in the limits $n \to \pm\infty$ of the recurrence relation, it is evident that once we find a solution of Eq. (2·21), it can be used to generate homogeneous solutions irrespective of whether it is real or complex. In this section, we confirm this by using the luminosity of gravitational waves radiated by a particle in a circular, equatorial orbit around a Kerr black hole. The complete formulas are given in Appendix A of paper I. We compare the numerical

Table III.   Table of ν for various values of $M\omega$ in the case $q = 0.99$ and -0.99, $s = -2$, $l = m = 2$.

$M\omega$	$q = 0.99$		$q = -0.99$	
	$\mathrm{Re}(\nu)$	$\mathrm{Im}(\nu)$	$\mathrm{Re}(\nu)$	$\mathrm{Im}(\nu)$
0.10	1.9806255500899	0.0000000000000	1.9778681909419	0.0000000000000
0.20	1.9239618344032	0.0000000000000	1.8984257752783	0.0000000000000
0.30	1.8183581833078	0.0000000000000	1.6857218860079	0.0000000000000
0.31	1.8027568870615	0.0000000000000	1.6371352569052	0.0000000000000
0.32	1.7854692988454	0.0000000000000	1.5499916877959	0.0000000000000
0.33	1.7660512947108	0.0000000000000	1.5000000000000	0.1201460888531
0.34	1.7438484200603	0.0000000000000	1.5000000000000	0.1788957377084
0.35	1.7178247791233	0.0000000000000	1.5000000000000	0.2240840951862
0.36	1.6861420552899	0.0000000000000	1.5000000000000	0.2628158063725
0.37	1.6447942140179	0.0000000000000	1.5000000000000	0.2976343179397
0.38	1.5793009665553	0.0000000000000	1.5000000000000	0.3297922470347
0.39	1.5000000000000	0.0974489094430	1.5000000000000	0.3600132102046
0.40	1.5000000000000	0.1628152952473	1.5000000000000	0.3887584134857
0.50	1.5000000000000	0.5368498162041	1.5000000000000	0.6365360949922
0.60	1.5000000000000	0.8672067267975	1.5000000000000	0.8571228112204
0.70	1.5000000000000	1.1838651090370	1.5000000000000	1.0704661825964
0.80	1.5000000000000	1.4840266489876	1.5000000000000	1.2821245153699
0.90	1.5000000000000	1.7701386563708	1.5000000000000	1.4938849397247
1.00	1.5000000000000	2.0454330629622	1.5000000000000	1.7061371538867
1.10	1.5000000000000	2.3125401729619	1.5000000000000	1.9187278288162
1.20	1.5000000000000	2.5734029380085	1.5000000000000	2.1313317677628
1.30	1.5000000000000	2.8294329783970	1.5000000000000	2.3436142271920
1.40	1.5000000000000	3.0816629547228	1.5000000000000	2.5552922279595
1.50	1.5000000000000	3.3308588672551	1.5000000000000	2.7661482256677
1.60	1.5000000000000	3.5775977157128	1.5000000000000	2.9760238443012
1.70	1.5000000000000	3.8223206679586	1.5000000000000	3.1848072932141
1.80	1.5000000000000	4.0653697494531	1.5000000000000	3.3924204618486
1.90	1.5000000000000	4.3070135210021	1.5000000000000	3.5988078524059
2.00	1.5000000000000	4.5474653357747	1.5000000000000	3.8039277638612
2.10	1.5000000000000	4.7868965237373	1.5000000000000	4.0077454471779
2.20	1.5000000000000	5.0254460525305	1.5000000000000	4.2102277404164
2.30	1.5000000000000	5.2632277012574	1.5000000000000	4.4113386736802
2.40	1.5000000000000	5.5003354519402	1.5000000000000	4.6110355696752
2.50	1.5000000000000	5.7368475857391	1.5000000000000	4.8092651925867
2.60	1.5000000000000	5.9728298259083	1.5000000000000	5.0059594834575
2.70	1.5000000000000	6.2083377711225	1.5000000000000	5.2010303381768
2.80	1.5000000000000	6.4434187950814	1.5000000000000	5.3943626971054
2.90	1.5000000000000	6.6781135409542	1.5000000000000	5.5858048534288
3.00	1.5000000000000	6.9124571056503	1.5000000000000	5.7751542098469

data with those computed with the numerical integration method of Kennefick.[*]

The innermost stable circular orbit (ISCO) around a Kerr black hole is given by

$$r_{\mathrm{ISCO}} = M[3 + Z_2 \mp \sqrt{(3 - Z_1)(3 + Z_1 + 2Z_2)}], \tag{4.1}$$

$$Z_1 = 1 + (1 - q^2)^{1/3}[(1 + q)^{1/3} + (1 - q)^{1/3}], \tag{4.2}$$

---

[*] The numerical data were kindly provided to us by D. Kennefick and are based on the work presented in Ref. 11).

$$Z_2 = \sqrt{3q^2 + Z_1^2},$$
(4·3)

Table IV.   Table of ν for various values of $M\omega$ in the case $s = 0$, $l = m = 2$ and $q = 0$.

$M\omega$	$\mathrm{Re}(\nu)$	$\mathrm{Im}(\nu)$
0.1000	1.9848275014852	0.0000000000000
0.2000	1.9376748241581	0.0000000000000
0.3000	1.8522206563655	0.0000000000000
0.4000	1.7069234201112	0.0000000000000
0.4100	1.6861876869380	0.0000000000000
0.4200	1.6631943548601	0.0000000000000
0.4300	1.6369668328189	0.0000000000000
0.4400	1.6053426169451	0.0000000000000
0.4500	1.5608220358616	0.0000000000000
0.4600	1.5000000000000	0.0580486824445
0.4700	1.5000000000000	0.1001804231496
0.4800	1.5000000000000	0.1273338678120
0.4900	1.5000000000000	0.1476523972303
0.5000	1.5000000000000	0.1633287233824
0.5100	1.5000000000000	0.1751890776086
0.5200	1.5000000000000	0.1834763247507
0.5300	1.5000000000000	0.1880516714671
0.5400	1.5000000000000	0.1883986754070
0.5500	1.5000000000000	0.1834683228152
0.5600	1.5000000000000	0.1712231357384
0.5700	1.5000000000000	0.1472113005187
0.5800	1.5000000000000	0.0974051775175
0.5900	1.5967266037405	0.0000000000000
0.6000	1.6978839941760	0.0000000000000
0.6040	1.7370771353709	0.0000000000000
0.6080	1.7796485136225	0.0000000000000
0.6120	1.8295192010822	0.0000000000000
0.6160	1.8982359899500	0.0000000000000
0.6200	2.0000000000000	0.0881232882027
0.6600	2.0000000000000	0.4182708018765
0.7000	2.0000000000000	0.5798590491029
0.8000	2.0000000000000	0.8682632610900
0.9000	2.0000000000000	1.0958382861914
1.0000	2.0000000000000	1.2916407295318
1.1000	2.0000000000000	1.4596540676691
1.2000	2.0000000000000	1.5871735288388
1.3000	2.0000000000000	1.5757480036493
1.4000	1.5000000000000	1.8980859589471
1.6000	1.5000000000000	2.5246610689374
1.8000	1.5000000000000	3.0134306373653
2.0000	1.5000000000000	3.4652896348154
2.2000	1.5000000000000	3.8988668745912
2.4000	1.5000000000000	4.3212911554702
2.6000	1.5000000000000	4.7360933390574
2.8000	1.5000000000000	5.1452723630699
3.0000	1.5000000000000	5.5500484659006

where the upper and lower signs refer to the cases $q > 0$ and $q < 0$, respectively. The orbital angular frequency of a circular orbit is given by

$$\Omega = \frac{M^{1/2}}{r^{3/2}(1 + q(M/r)^{3/2})}. \quad (4·4)$$

The angular frequency of gravitational waves corresponding to the harmonic m is given by $\omega = m\Omega$. For $q > 0$, the orbital radius of the ISCO becomes smaller than that in the Schwarzschild case, and it approaches the event horizon as $q \to 1$. Thus, $M\omega$ around the ISCO can be larger than $(M\omega)_{\max}$.

In Table VII, we list the numerical data for the gravitational wave luminosity induced by a particle in a circular orbit in the case that $M\omega$ is larger than $(M\omega)_{\max}$. We find that the numerical data computed using a complex ν agree with those computed using the numerical integration method to about 5 or 6 digits. This is approximately the same degree of accuracy of the numerical integration. This demonstrates the validity of using a complex ν to produce the homogeneous solutions of the Teukolsky equation.

In the case of eccentric orbits, there are infinite number of higher harmonics for each l, m. Thus, in principle, there are many harmonics for which $M\omega$ is larger than $(M\omega)_{\max}$. Here, we estimate the range of harmonics needed to express the total power of the gravitational waves with the relative error less than 10^{-5} using the Newtonian, quadrupole approximation, in the case of a non-spinning binary. The power radiated in nth harmonics is given by[12]
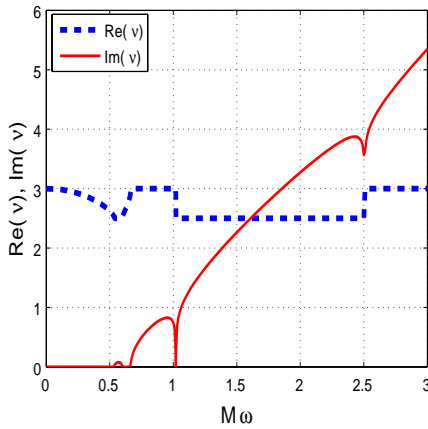
Fig. 8. The values of the real and imaginary parts of ν as functions of $M\omega$ in the case $s = -2$, $l = m = 3$ and $q = 0$.
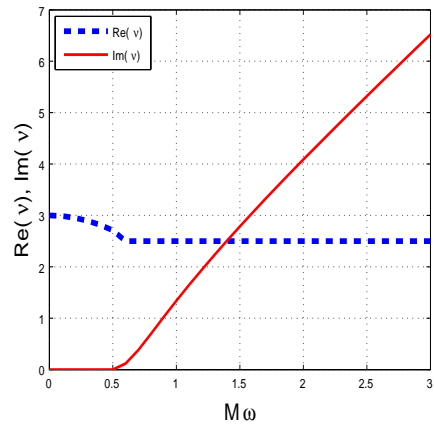

Fig. 9. The values of the real and imaginary parts of ν as functions of $M\omega$ in the case $s = -2$, $l = m = 3$ and $q = 0.99$.
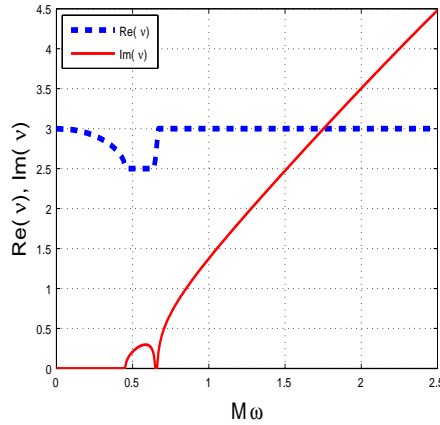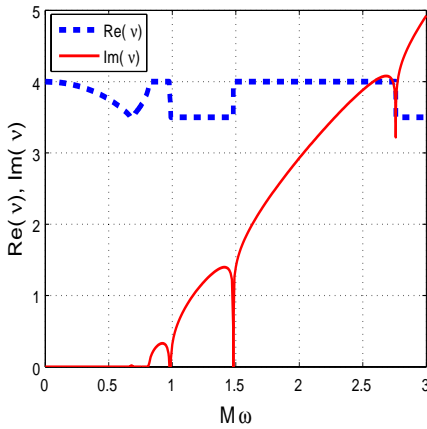

Fig. 10. The values of the real and imaginary parts of ν as functions of $M\omega$ in the case $s = -2$, $l = m = 3$ and $q = -0.99$.

$$P(n) = \frac{32}{5} \frac{m_1^2 m_2^2 (m_1 + m_2)}{r_a^5} g(n, e), \qquad (4\cdot5)$$

where m_1 and m_2 are the masses of the two stars forming the binary, e is the eccentricity, r_a is the semi-major axis of the orbit, and we have

$$g(n, e) = \frac{n^4}{32} \Bigg\{ \left[J_{n-2}(ne) - 2e J_{n-1}(ne) + \frac{2}{n} J_n(ne) + 2e J_{n+1}(ne) - J_{n+2}(ne) \right]^2$$

$$+ (1 - e^2)[J_{n-2}(ne) - 2J_n(ne) + J_{n+2}(ne)]^2 + \frac{4}{3n^2}(J_n(ne))^2 \Bigg\}, \qquad (4\cdot6)$$

Fig. 11. The values of the real and imaginary parts of ν as functions of $M\omega$ in the case $s = -2$, $l = m = 4$ and $q = 0$.
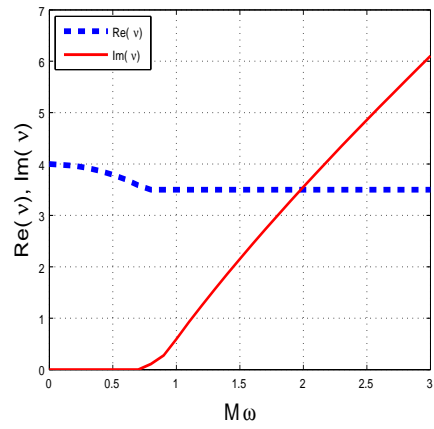

Fig. 12. The values of the real and imaginary parts of ν as functions of $M\omega$ in the case $s = -2$, $l = m = 4$ and $q = 0.99$.
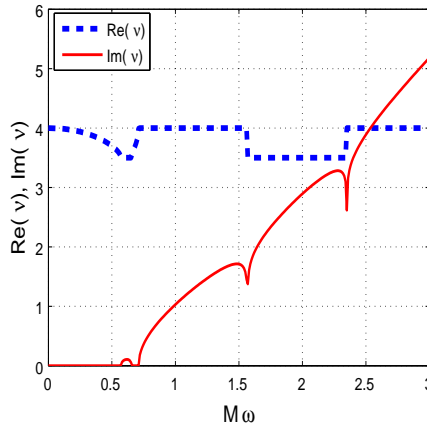

Fig. 13. The values of the real and imaginary parts of ν as functions of $M\omega$ in the case $s = -2$, $l = m = 4$ and $q = -0.99$.

where $J_n(z)$ is the Bessel function. The angular frequency for each harmonic is given by $\omega = n\omega_0$, with $\omega_0 = (m_1 + m_2)^{1/2}/r_a^{3/2}$. In Fig. 16, we plot the contours of the values of $M\omega$ that must be included in the total power as functions of e and r_a. We find that for small r_a, there is a relatively wide range of values of e for which the required value of $M\omega$ exceeds $(M\omega)_{\max} = 0.36$ in the case $l = m = 2$ and $q = 0$. In such cases, complex ν must be employed in order to evaluate the gravitational radiation. Of course, we should keep in mind that, because this is based on the Newtonian, quadrupole approximation, this result will be changed quantitatively in the case of fully relativistic treatment.
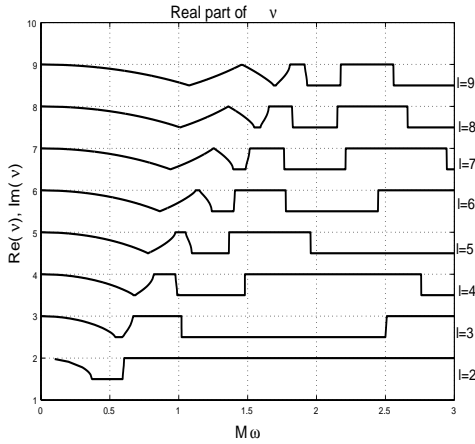
Fig. 14. The values of the real parts of ν as functions of $M\omega$ in the cases $l = 2, 3, \cdots, 9$, $s = -2$ and $q = 0$.
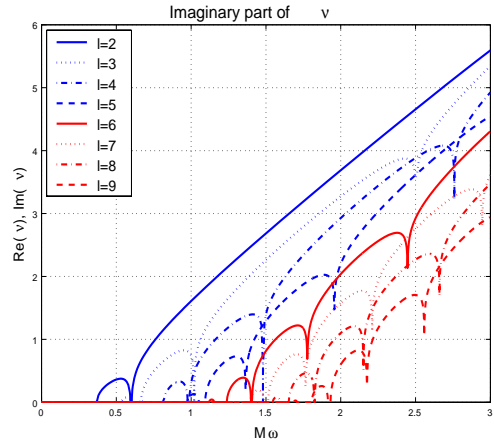

Fig. 15. The values of the imaginary parts of ν as functions of $M\omega$ in the cases from $l = 2, 3, \cdots, 9$, $s = -2$ and $q = 0$.
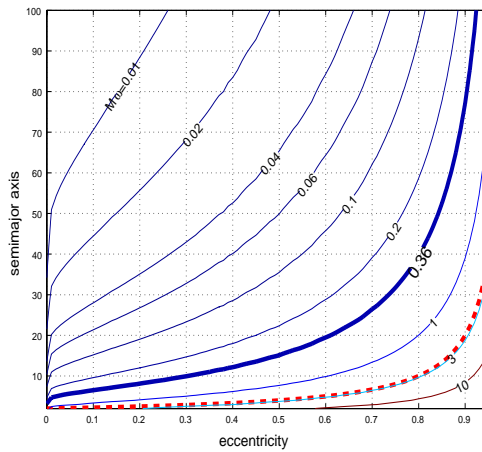

Fig. 16. The contours of the values of $M\omega(= Mn\omega_0)$ that must be included in the evaluation of the total power in order to obtain the the relative error less than 10^{-5}. Here, $M = m_1 + m_2$. The thick curve corresponds to the contour for $M\omega = 0.36$, which is equal to $(M\omega)_{\max}$, in the case $l = m = 2$ and $q = 0$, above which ν becomes complex. The region under thick dashed curve should be excluded from consideration, because there, the pericenter distance is less than $2M$. Thus, in the region between the thick curve and the thick dashed curve, the parameter ν can have a complex value.

§5. Summary and discussion

We have investigated the numerical properties of the solutions of the continued fraction equation derived by Leaver and Mano et al. in the formalism of the analytic representation of the homogeneous solution of the Teukolsky equation. We have found that, for each s, l, m and q, the solution ν takes a real or complex value, depending on the value of ω. We have also found that, when ν is complex, its real

Table V. Table of ν for various values of $M\omega$ in the case $s = 0$, $l = m = 2$ and $q = 0.99$.

$M\omega$	Re(ν)	Im(ν)
0.10	1.9855006468982	0.0000000000000
0.20	1.9433423104280	0.0000000000000
0.30	1.8738919793067	0.0000000000000
0.40	1.7745498379081	0.0000000000000
0.50	1.6249603205669	0.0000000000000
0.51	1.6016482354182	0.0000000000000
0.52	1.5720774742602	0.0000000000000
0.53	1.5140777829215	0.0000000000000
0.54	1.5000000000000	0.0683318312500
0.55	1.5000000000000	0.0970789832967
0.56	1.5000000000000	0.1187106486632
0.57	1.5000000000000	0.1367752823053
0.58	1.5000000000000	0.1526950899429
0.59	1.5000000000000	0.1672593963838
0.60	1.5000000000000	0.1809982771760
0.70	1.5000000000000	0.3387878153683
0.80	1.5000000000000	0.5844007364833
0.90	1.5000000000000	0.8212346456388
1.00	1.5000000000000	0.9679578324407
1.10	2.0000000000000	1.0719514201554
1.20	2.0000000000000	1.5606928653937
1.30	2.0000000000000	1.8822793013188
1.40	2.0000000000000	2.1581224329993
1.50	2.0000000000000	2.4081352814494
1.60	2.0000000000000	2.6392239009791
1.70	2.0000000000000	2.8536938783809
1.80	2.0000000000000	3.0506896346940
1.90	2.0000000000000	3.2246989210551
2.00	2.0000000000000	3.3561709666536
2.10	2.0000000000000	3.2904400721719
2.20	1.5000000000000	3.7368758127391
2.30	1.5000000000000	4.0811236068986
2.40	1.5000000000000	4.3637677117354
2.50	1.5000000000000	4.6216867037460
2.60	1.5000000000000	4.8652774867248
2.70	1.5000000000000	5.0989848264810
2.80	1.5000000000000	5.3251065286991
2.90	1.5000000000000	5.5449488222337
3.00	1.5000000000000	5.7592716343452

Table VI. Table of ν for various values of $M\omega$ in the case $s = 0$, $l = m = 2$ and $q = -0.99$.

$M\omega$	Re(ν)	Im(ν)
0.10	1.9840980928918	0.0000000000000
0.20	1.9308382464262	0.0000000000000
0.30	1.8203733727014	0.0000000000000
0.31	1.8041051082066	0.0000000000000
0.32	1.7863405245509	0.0000000000000
0.33	1.7667869072726	0.0000000000000
0.34	1.7450236585402	0.0000000000000
0.35	1.7204062673298	0.0000000000000
0.36	1.6918506722768	0.0000000000000
0.37	1.6572410906180	0.0000000000000
0.38	1.6110789879720	0.0000000000000
0.39	1.5000000000000	0.0186032751635
0.40	1.5000000000000	0.1154238436610
0.50	1.5000000000000	0.3965366549457
0.60	1.5000000000000	0.5628860942422
0.70	1.5000000000000	0.6786359420169
0.80	1.5000000000000	0.6765122702806
0.90	2.0000000000000	0.9125809354487
1.00	2.0000000000000	1.2541180907051
1.10	2.0000000000000	1.5100321536697
1.20	2.0000000000000	1.7355022863878
1.30	2.0000000000000	1.9421454082317
1.40	2.0000000000000	2.1324040070446
1.50	2.0000000000000	2.3031629738421
1.60	2.0000000000000	2.4408891644519
1.70	2.0000000000000	2.4732101098580
1.80	1.5000000000000	2.7185951268120
1.90	1.5000000000000	3.0969911535975
2.00	1.5000000000000	3.3873306639375
2.10	1.5000000000000	3.6492406015533
2.20	1.5000000000000	3.8963211129597
2.30	1.5000000000000	4.1339652371712
2.40	1.5000000000000	4.3648798107882
2.50	1.5000000000000	4.5906202696084
2.60	1.5000000000000	4.8121617032199
2.70	1.5000000000000	5.0301522240344
2.80	1.5000000000000	5.2450395718077
2.90	1.5000000000000	5.4571399180362
3.00	1.5000000000000	5.6666774973656

part is always an integer or half integer. Although there are certain regularities in the behavior of the solution, we have not determined how such behavior is controlled by the continued fraction equation. We hope to investigate the behavior of ν analytically in the future.

In order to confirm the existence of complex ν, we have computed the gravitational wave luminosity emitted by a particle in circular, equatorial orbit around a Kerr black hole in the case that ν is complex, and compared the results with those

Table VII. Comparison of the energy fluxes obtained using the numerical integration method of Kennefick and the method presented here in the case $r_0 = 1.55M$ and $q = 0.99$, with complex ν.

l	m	$\mathrm{Re}(\nu)$	$\mathrm{Im}(\nu)$	Numerical integration	This paper	Relative error
2	2	1.5	1.1374192131794	$3.568050135 \times 10^{-2}$	$3.568033154338851 \times 10^{-2}$	4.76×10^{-6}
3	3	2.5	1.4249576682707	$2.152962111 \times 10^{-2}$	$2.152959342790158 \times 10^{-2}$	1.29×10^{-6}
4	4	3.5	1.7677955367662	$1.230541176 \times 10^{-2}$	$1.230541952573211 \times 10^{-2}$	6.31×10^{-7}
5	4	4.5	0.3735768429955	$1.933923538 \times 10^{-5}$	$1.933924400940079 \times 10^{-5}$	4.46×10^{-7}
5	5	4.5	2.1437000387424	$7.259841388 \times 10^{-3}$	$7.259849874157195 \times 10^{-3}$	1.17×10^{-6}
6	5	5.5	0.8032470628900	$1.536518877 \times 10^{-5}$	$1.536520289551414 \times 10^{-5}$	9.19×10^{-7}
6	6	5.5	2.5395166388946	$4.404590776 \times 10^{-3}$	$4.404599359654937 \times 10^{-3}$	1.95×10^{-6}
7	6	6.5	1.2521347909128	$1.148793520 \times 10^{-5}$	$1.148795883734041 \times 10^{-5}$	2.06×10^{-6}
7	7	6.5	2.9481395894691	$2.726943363 \times 10^{-3}$	$2.726949666682515 \times 10^{-3}$	2.31×10^{-6}
8	7	7.5	1.6997166387020	$8.267139284 \times 10^{-6}$	$8.267168128593364 \times 10^{-6}$	3.49×10^{-6}
8	8	7.5	3.3654788843469	$1.713109264 \times 10^{-3}$	$1.713110726903289 \times 10^{-3}$	8.54×10^{-7}
9	7	8.5	0.3781387034254	$1.650193407 \times 10^{-7}$	$1.650193971262395 \times 10^{-7}$	3.42×10^{-7}
9	8	8.5	2.1467598463840	$5.800131555 \times 10^{-6}$	$5.800152000099428 \times 10^{-6}$	3.53×10^{-6}
9	9	8.5	3.7890216134824	$1.087833559 \times 10^{-3}$	$1.087830324625970 \times 10^{-3}$	2.97×10^{-6}
10	8	9.5	0.8445521091574	$1.423932484 \times 10^{-7}$	$1.423939557356283 \times 10^{-7}$	4.97×10^{-6}
10	9	9.5	2.5936449978532	$3.998328655 \times 10^{-6}$	$3.998328388790399 \times 10^{-6}$	6.66×10^{-8}
10	10	9.5	4.2171390613851	$6.963970144 \times 10^{-4}$	$6.963929698290593 \times 10^{-4}$	5.81×10^{-6}

computed using a numerical integration method. We found that the two results are consistent. This shows clearly the validity of the existence of complex ν. Even if $M\omega$ becomes larger than a certain critical value and a real ν does not exist, we can use the MST formalism by treating ν as a complex value. Thus, the region of ω in which the MST formalism can be used becomes much wider than in the case that we consider only real ν, as in paper I.

There is, however, a limitation on the values of ω for which we can use the MST formalism for actual numerical computations. When $M\omega$ becomes very large (say $M\omega > 5$ in the case $s = -2$, $l = 2$ and $q = 0$), it becomes very difficult to evaluate the continued fraction equation (2·21) accurately because of the loss of accuracy. As ω becomes large, β_n approaches $-(\alpha_n^\nu R_{n+1} + \gamma_n^\nu L_{n-1})$ irrespective of ν. Thus, it becomes difficult to evaluate Eq. (2·21) numerically with high accuracy. We must solve this problem because $M\omega$ becomes very large in the cases of generic orbits, which are important for the data analysis for LISA. A possible solution is to derive the high frequency expansion of ν. If we cannot solve the problem, we may need to use numerical integration methods to evaluate the homogeneous solutions of the Teukolsky equation when $M\omega$ becomes very large. However, we believe that the MST method supplemented by some numerical integration is a very powerful method for the numerical computation of the Teukolsky equation.

Based on the analysis presented in this paper, we plan to apply the MST formalism to the evaluation of the gravitational wave luminosity in the cases of eccentric orbits and more generic, non-equatorial orbits, and to investigate the data analysis issue for LISA in the near future.

Acknowledgements

References

1) LISA web page: `http://lisa.jpl.nasa.gov/`
2) J. R. Gair, L. Barack, T. Creighton, C. Cutler, S. L. Larson, E. S. Phinney and M. Vallisneri, Class. Quantum Grav. **21** (2004), S1595.
3) S. A. Teukolsky, Astrophys. J. **185** (1973), 635.
4) R. Fujita and H. Tagoshi, Prog. Theor. Phys. **112** (2004), 415. (Paper I)
5) S. Mano, H. Suzuki and E. Takasugi, Prog. Theor. Phys. **95** (1996), 1079.
6) E. W. Leaver, J. Math. Phys. **27** (1986), 1238.
7) S. Mano and E. Takasugi, Prog. Theor. Phys. **97** (1996), 213.
8) Ed. M. Abramowitz and I. A. Stegun, *Handbook of Mathematical Functions* (Dover, New York, 1972).
9) M. Sasaki and H. Tagoshi, Living Rev. Relativity **6** (2003), 6; `http://www.livingreviews.org/lrr-2003-6/`
10) W. Gautschi, S. I. A. M. Review **9** (1967), 24.
11) K. Glampedakis and D. Kennefick, Phys. Rev. D **66** (2002), 044002.
12) P. C. Peters and J. Mathews, Phys. Rev. **131** (1963), 435.